Determination of the complex refractive indices of aerosol from aerodynamic particle size spectrometer and integrating nephelometer measurements

Yong Han,[1,2,*] Daren Lü,[1,2] Ruizhong Rao,[3] and Yingjian Wang[3]

[1]School of Atmospheric Sciences, Nanjing University, Nanjng, 210093, China

[2]Key Laboratory of Middle Atmosphere and Global Environment Observation, Institute of Atmospheric Physics, Chinese Academy of Sciences, P.O. Box 9804, Beijing 100029, China

[3]Key Laboratory of Atmospheric Composition and Optical Radiation, Anhui Institute of Optics and Fine Mechanics, Chinese Academy of Sciences, P.O. Box 1125, Hefei 230031, China

*Corresponding author: HanYong@nju.edu.cn

Received 6 November 2008; revised 21 June 2009; accepted 21 June 2009; posted 24 June 2009 (Doc. ID 103609); published 13 July 2009

An approach is developed to retrieve the complex index of refraction by coupling two well known instruments: an aerodynamic particle size spectrometer (APS) probe for measuring aerosol size distributions and an integrating nephelometer for measuring total light scattering coefficients. The retrieval is realized by an iterative least squares minimization of the fractional error between the nephelometer-measured light scattering coefficients and those calculated from the APS-measured size distributions based on the Mie theory for spherical particles. High-resolution data collected during two field experiments conducted at two locations with distinct environments in China are analyzed. The results show that light scattering coefficients, aerosol size distributions, and refractive indices all vary substantially with time. Further examination of their dependence on relative humidity suggests that instead of being monotonic change with relative humidity, the refractive index often fluctuates when the relative humidity changes. This nonmonotonic variation of refractive index with relative index suggests concurrent change of relative humidity and other chemical compositions. Possible errors in the retrieval are also discussed.

OCIS codes: 010.1100, 010.1110, 290.1090, 290.3030, 290.5850, 120.5710.

1. Introduction

Atmospheric aerosols affect the Earth's radiation budget and climate, both directly through the processes of scattering and absorption of solar and thermal infrared radiation and indirectly via modifying cloud properties [1–10]. Light scattering and absorbing properties of aerosol particles also strongly influence light propagation in the atmosphere; especially, absorption can cause high-energy laser beam thermal and air breakdown [11–15]. Fundamental to the optical properties of atmospheric aerosols is the complex index of refraction,

$$m = m_r - im_i, \tag{1}$$

where the real part m_r and the imaginary part m_i primarily determine light scattering and absorbing properties of aerosol particles, respectively. In particular, it has been recognized that the value of m_i is essential to determining aerosol absorption properties and hence radiation balance in the atmosphere [2,16,17]. For example, Yamamoto and Tanaka [18]

0003-6935/09/214108-10$15.00/0

showed that an increase of aerosol loading in the atmosphere could lead to a cooling or warming effect on the Earth's climate depending on the value of m_i (cooling when $m_i < 0.050$, but warming when $m_i \geq 0.050$). Absorbing aerosols such as soot are also known to exert a so-called warming effect on climate [19].

In view of its importance, much effort has been devoted to developing approaches for measuring aerosol absorption and refractive indices of aerosol particles [20–33]. In general, instruments for measuring light absorption can be classified into three types according to their detection principles. The first type of instrument is based on the photoacoustic principle [34]. Aerosol-induced light absorption heats the surrounding air, leading to sound waves. When the high energy incident light is used to improve sensitivity of measurements, some components of aerosol particles are evaporated, and then there will be an error term introduced [35]. The second type of instrument measures absorption coefficients of aerosol samples by integrating slicing [21,36]. This method has been widely used due to its simplicity and easy implementation [28]. A shortcoming of this method is that the optical properties of particles collected on the filter membrane may be different from those in the real atmosphere. In addition, the method also ignores the influences of multiscattering and backscattering, as well as some boundary layer effect. The third type of instrument determines absorption properties by measuring the carbon element in atmospheric aerosols and then relates the amount of carbon to light absorption. Then, the imaginary part of complex refractive index can be obtained by absorption coefficients from Mie theory. Obviously, the accuracy of the carbon element method depends on two conditions, that the carbon content is accurately measured, and that the mass absorption efficiency of carbon is known. Unfortunately, these two conditions are usually difficult to meet in practice [7,28].

The refractive index is related to the chemical compositions of aerosol particles, and often depends on the light wavelength. Measuring refractive indices of aerosol particles is even more challenging and often involves solving some inverse problems. For example, Romanov *et al.* [25] proposed an inversion method that simultaneously retrieves the aerosol refractive index and particle size distribution from ground-based measurements of direct and scattered solar radiation. Zhao *et al.* [23,24] developed a method that combines the light scattering measurements with a polar nephelometer, and particle size distributions with an optical particle counter (OPC). Liu and Daum [29] proposed a method that infers the real part of refractive index and corrects for the difference in the refractive indices between the ambient aerosols and the latex particles used to calibrate the optical particle counter by coupling the nephelometer and OPC measurements. The Liu–Daum method was extended to retrieve the imaginary part of the refractive index by Guyona *et al.* [30]. Hand and Kreidenweis developed one method for retrieving particle refractive index and effective density from aerosol size distribution data by using a TSI differential mobility analyzer (DMA), a PMSLASAIR 1003 OPC, and a TSI APS 3320 [31].

Despite the valuable results obtained previously, our knowledge of the complex refractive index of the atmospheric aerosol particles is still very limited. Especially, high-resolution, long-term measurements of refractive indices and their wavelength dependence have been rarely investigated, hindering further progress in many areas such as climate change and free space laser communication. To address these important yet poorly studied issues, this work takes advantage of concurrent long-term measurements of light scattering by a three-wavelength integrating nephelometer and of aerosol size distributions by an aerodynamic particle size spectrometer (APS, TSI model 3321). The complex refractive index is inverted from the combined measurements of light scattering coefficients and size distributions using a method that is similar to those reported in [24,29,30].

The paper is organized as follows. The physical basis of the method and the instrumentation are presented in Section 2. The major results and discussions are presented in Section 3. Concluding remarks are made in Section 4.

2. Field Experiments, Instrumentation, and Retrieval Method

Field experiments were done in Xiamen (118.04E, 24.26N) and Hefei (117.16E, 31.51N) of China. Xiamen is a coastal city, and the experimental position in Xiamen is about 20 m distance from the seacoast. Hefei is an inland city, lying in mideastern China. The aerosol types of the two sites are typical oceanic aerosols (Xiamen) and inland aerosols (Hefei), respectively. The sampling locations were about 4 m and 5 m above ground level in Hefei and in Xiamen, respectively. The sampling periods of APS and integrating nephelometer were per minute with synchronous sampling. The experiments provided aerosol optical parameters for our test of free space laser communication in 2005.

A. Instrumentation

Figure 1 shows the main instruments used in our field experiments. The APS measures aerosol size distribution by determining the time-of-flight of individual particles in an accelerating flow field, which is calibrated by polystyrene gum elastic. The APS can convert particle flight time measured each time into aerodynamic diameter. A complete particle size distribution may be determined in a matter of seconds or minutes, making the APS a good choice for a broad range of applications [37–39]. The dimension of its detection diameter is from 0.5 to 20 μm, and the measurement accuracy of concentration is $\pm 10\%$.

The scanning mobile particle sizer (SMPS, TSI model 3936) is composed of an electrostatic classifier

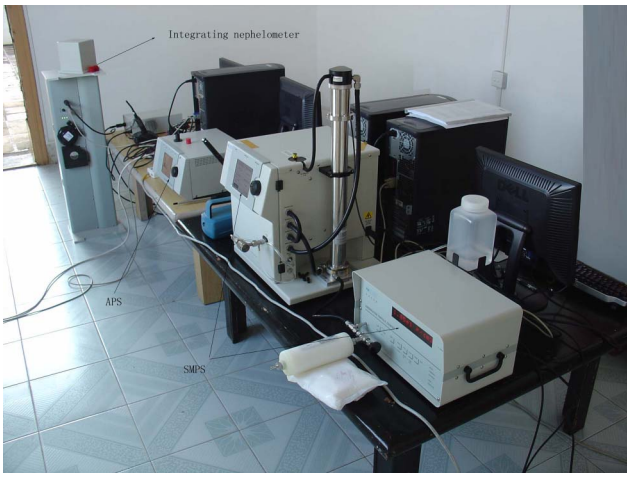

Fig. 1. Instruments in our experiments.

(TSI model 3080), a condensation particle counter (CPC, TSI model 3022A), and a long differential mobile analyzer (LDMA) [40–42]. The concentration range of SMPS is from 2 to 10^8 particles/cm^3, the particle diameter range of SMPS is from 7 to 1000 nm, and the measurement cycle time of SMPS is from 60 to 600 s. We selected 60 s in our experiments.

The three-wavelength integrating nephelometer used in measurement of the aerosol total light scattering coefficient is manufactured by the TSI Company (Fig. 2). This integrating nephelometer simultaneously measures the light scattering coefficients of three wavelengths (450, 550, and 700 nm) with the scattering angles ranging from 7° to 170°. The average sampling time ranges from 1 to 4096 s (60 s in our experiments). The drift is less than 2.0×10^{-7} m^{-1} at 30 s, and the response time is less than 10 s. Note that nephelometers (integrating or polar) have proven to be reliable instruments for the measurement of light scattering coefficients of aerosols [35,43,44]. Nephelometers have also been used to measure visibility and aerosol optical depth in the atmospheric boundary layer and inverse size distributions in ground-based and airborne studies [45–62]. However, studies with integrating nephelometers are comparatively few in China, and most of these studies have concentrated mainly on the monitoring of light scattering coefficients of atmospheric aerosol and the optical properties of sand dust particles [63–67].

B. Retrieval Approach

The retrieval algorithm consists of two steps. First, the measured aerosol size distribution is used to generate an ensemble of total light scattering coefficients by varying the values of refractive index. The calculation is made for all three wavelengths of the nephelometer, and Mie theory for spherical particles is used in the calculation. Second, optimization is performed to locate the "optimal" value of refractive index with the method of least squares minimization of the error between the observed and calculated values of the scattering coefficients [68–71]. Briefly, the error function is given by

$$\delta_k = \left(\frac{1}{N} \sum_{i=1}^{N} \left[\frac{\beta_{\mathrm{sca}}|_{ki} - \beta_{\mathrm{aero}}|_{kj}}{\beta_{\mathrm{sca}}|_{ki}} \right]^2 \right)^{1/2}, \qquad (2)$$

where δ_k measures the fractional difference of the calculated total light scattering coefficients (β_{aero}) relative to that measured by the nephelometer (β_{sca}); N is the number of measurements used in the retrieval; the subscript k denotes the wavelength [$k =$

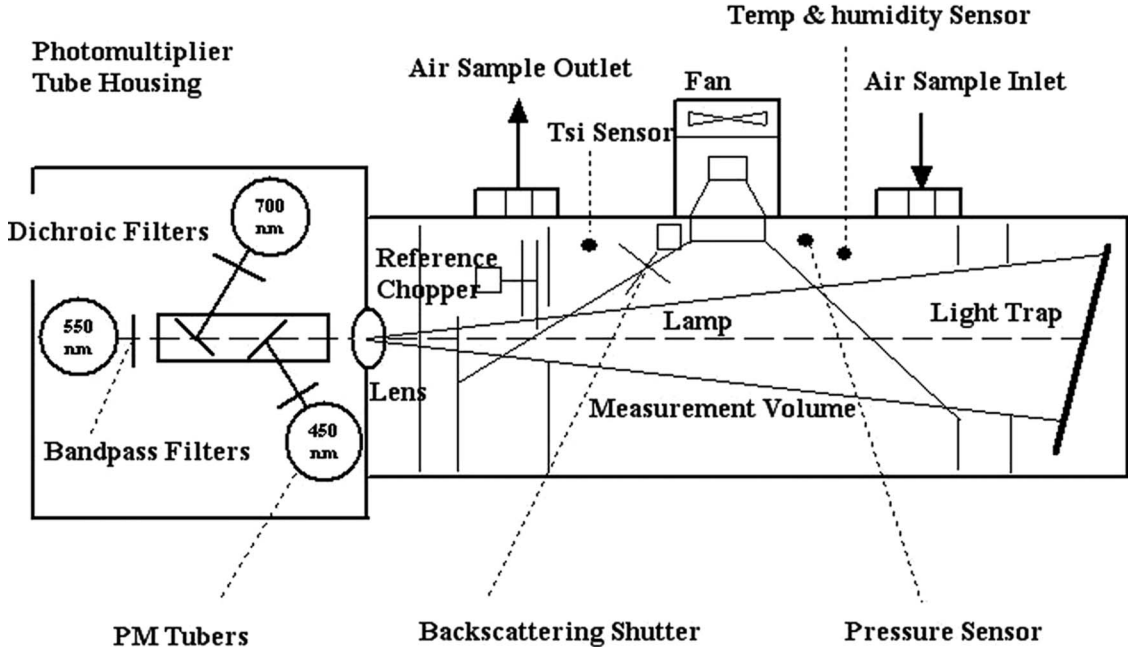

Fig. 2. Schematic diagram of the integrating nephelometer.

1 (450 nm), 2 (550 nm), 3 (700 nm)]. In the calculation, based on previous studies, the real part of refractive index varies from 1.3 (0.001) to 2.0, and the imaginary part changes from 10^{-6} to 1 with a logarithmic interval of 0.1. The optimal value of the refractive index is defined as that giving the minimum value of the error function.

This paper combines two instrument measurements (APS and integrating nephelometer) to determine the complex refractive indices in Xiamen and Hefei, China, where the environmental conditions are different. The APS and integrating nephelometer can implement measurements per minute. Especially, they do not require stable atmosphere conditions. Consequently, their measurements can be in response to changes of environments. Published studies with polar nephalometers in *Applied Optics* (for details, see Refs. [22–24]) stressed that the atmosphere needed to be stable and quiescent in order to apply the polar nephelometer technique, which could take periods from 15 to 30 minutes to obtain a sample measurement. As mentioned above, the method we used can improve the timeliness of the approach about determination of the refractive index, which will satisfy the requirements of some special optical projects.

3. Results

A. Temporal Variation

The measurements of light scattering coefficients and aerosol size distributions collected during the days of 16 and 30 June 2005 in Hefei and 4, 7, and 9 October 2005 in Xiamen are processed for refractive indices using the retrieval algorithm discussed above. Figures 3(a) and 3(b) show the scattering coefficients measured on 30 June in Hefei and 9 October in Xiamen in 2005, respectively. Figures 4(a) and 4(b) show the change ranges of size distribution at the same days as Figs. 3(a) and 3(b), respectively. It is anticipated that these temporal variations of the aerosol light scattering coefficients and size distributions will manifest themselves in the time series of the refractive indices.

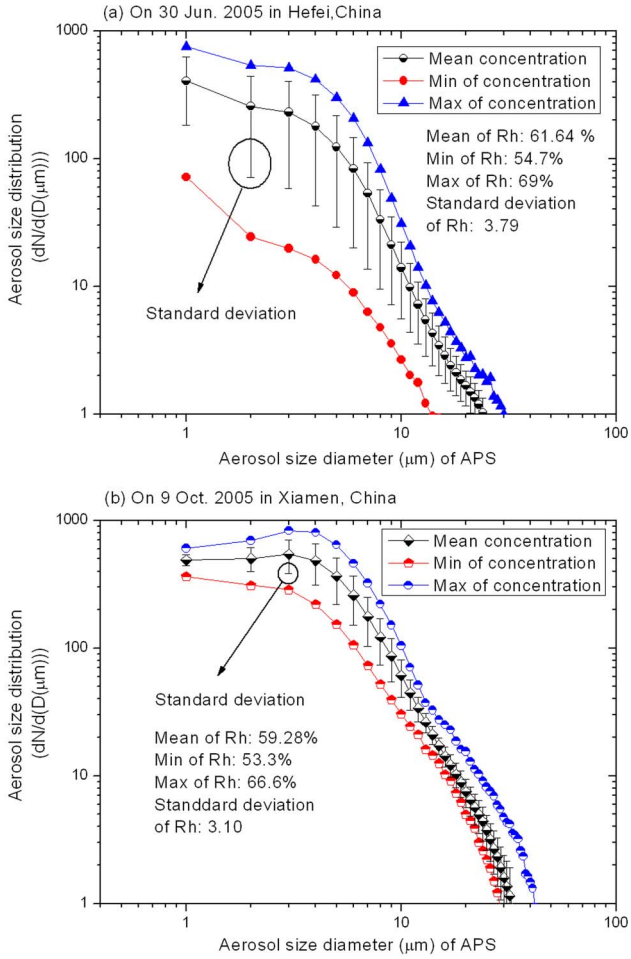

Fig. 4. (Color online) Change ranges of aerosol size distributions for the data measured (a) on 30 June 2005 in Hefei and (b) on 9 October 2005 in Xiamen, China.

Figure 5 depicts the temporal variation of the refractive indices retrieved according to the method described in Section 2. The statistical characteristics [e.g., the mean (M), standard deviation (SD), minimum (Min), and maximum (Max)] are also provided in the corresponding legends. An obvious feature of

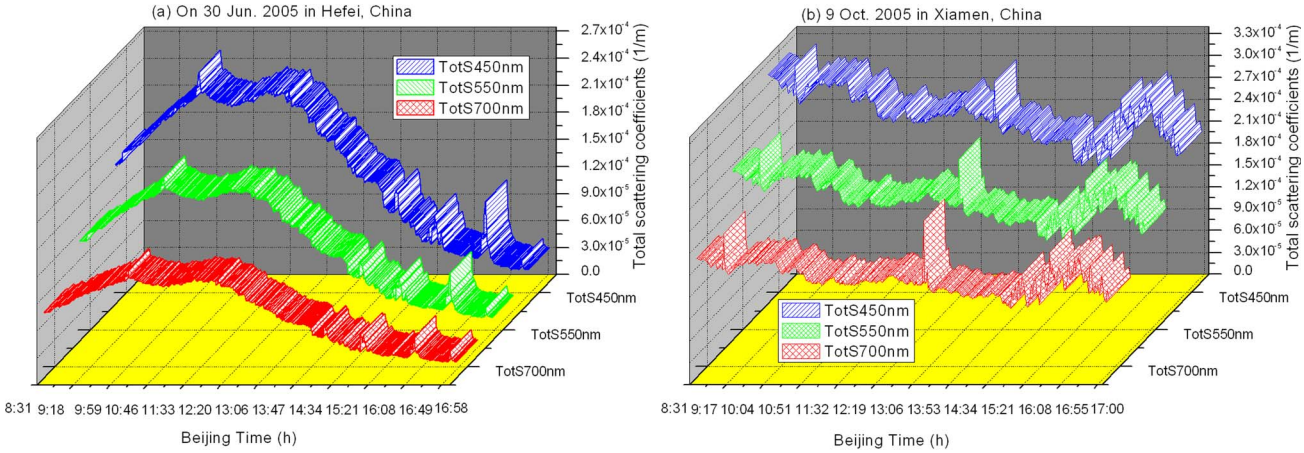

Fig. 3. (Color online) Aerosol scattering coefficients for data measured (a) on 30 June 2005 in Hefei and (b) on 9 October 2005 in Xiamen, China.

Fig. 5 is that the real and imaginary parts of the refractive index at both locations vary intermittently, instead of being a constant. It can be seen from Figs. 5(a) and 5(c) that the real part of the refractive index at 450 nm is less than that at 550 or 700 nm for most data points. The real refractive indices fluctuate wildly after 11:33 am in Hefei and after 12:55 pm in Xiamen, respectively. On the other hand, as shown in Figs. 5(b) and 5(d), the imaginary part of the refractive index exhibits an increasing trend with increasing wavelengths. Especially noteworthy is the abrupt decrease of the imaginary part after 14:13 pm in Xiamen [Fig. 5(d)]. Comparison between the two locations indicates that aerosol particles at Xiamen are more absorbing (the imaginary part is higher) than those at Hefei.

B. Effects of Relative Humidity

It has been long known that relative humidity (RH) is a major meteorological factor that affects aerosol size distributions, light scattering coefficients, and refractive indices [72]. This subsection further examines the relationships of the light scattering coefficient, the aerosol size distribution, and the refractive index to RH as embodied in the data. Figure 6 shows the light scattering coefficients as a function of RH measured (a) in Hefei and (b) in Xiamen. The data sets collected during 16 and 30 June 2005 at Hefei, and 4, 7, and 9 October 2005 at Xiamen are added to cover a wider range of RH. The interval of the RH is 3%, with the exception for the RH of 68% and 72%. At each RH, we selected three continuous measured points to retrieve complex refractive indices. It is noteworthy that instead of a monotonic increase of light scattering coefficients with increasing RH as expected from particle growth by vapor condensation, the light scattering coefficient varies widely and exhibits a minimum at RH of ~55% at Hefei, but RH of ~78% at Xiamen.

Figure 7 shows the aerosol size distributions averaged according to RH. It is clear that the aerosol size distributions are different when RH changes. In our retrieve method, the Lorentz expression is used to fit the aerosol size distributions for RH of ~68% to 90%, and the rest of the size distributions are fitted with the power-law expression. It is interesting to note

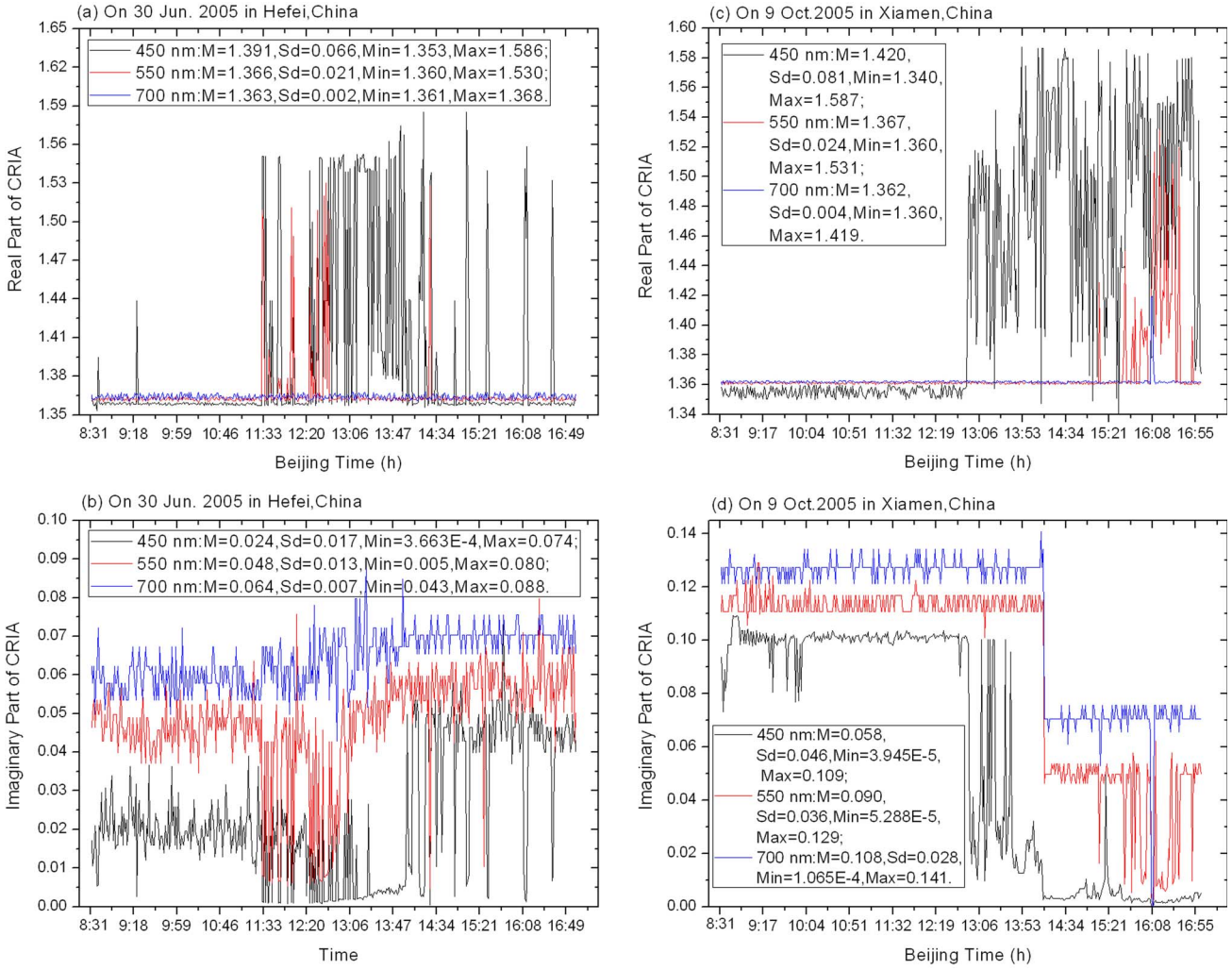

Fig. 5. (Color online) Temporal variation of the complex refractive indices of aerosol (CRIA). (a), (b) real and imaginary parts at Hefei, respectively; (c), (d) those in Xiamen, respectively.

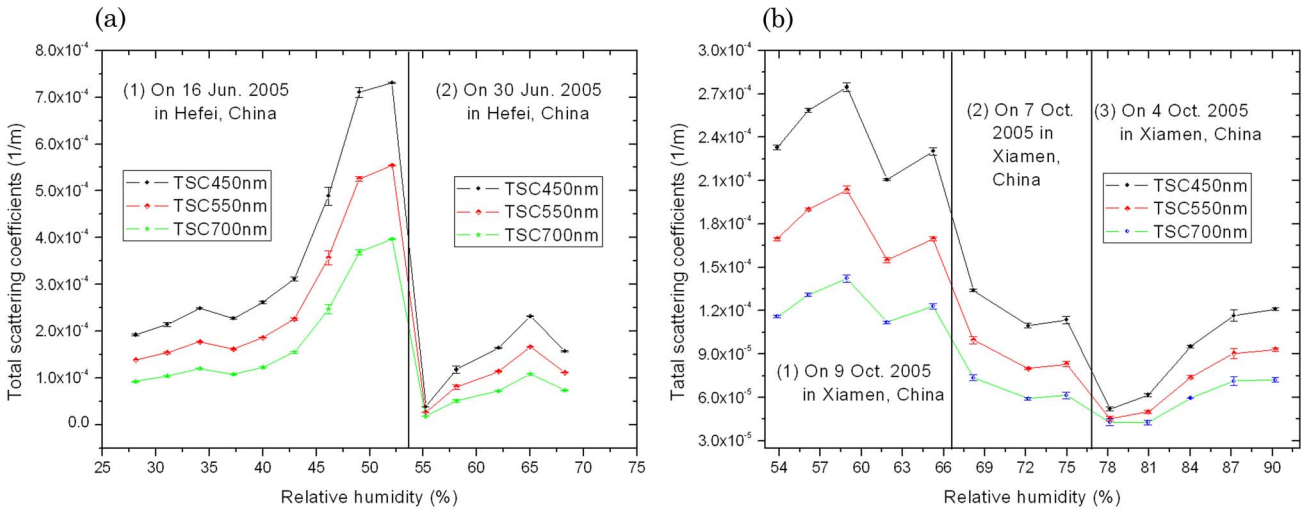

Fig. 6. (Color online) Aerosol total scattering coefficients in different RH for the data measured (a) on 16 and 30 June 2005 in Hefei and (b) on 4, 7, and 9 October 2005, in Xiamen, China, respectively.

that the size distributions at Hefei [Fig. 7(a)] appear to be at minimum when RH is ~55% (the green curve), but the minimum occurs around RH of ~78% at Xiamen, both in agreement with the minima of the corresponding light scattering coefficients shown in Fig. 6. Because the aerosol size distribution is a primary factor that determines the light scattering coefficient, the consistency of the two independent measurements suggests that the nonmonotonic variation with RH is real, at least for the data analyzed.

Figure 8 shows the refractive index as a function of RH. For the wavelengths of 450 and 550 nm, the real and imaginary parts of refractive indices fluctuate wildly at both Hefei and Xiamen. In contrast, at 700 nm, the real [Fig. 8(e)] and imaginary [Fig. 8(f)] parts are relatively stable, although extreme values appears around RH of ~49% at Hefei and RH of ~75% at Xiamen. These RH values appear near those where the minimal light scattering coefficients and aerosol concentration occur. The physics behind this phenomenon remains elusive and deserves further investigation. Generally speaking, the real part of refractive indices decreases with increasing wavelength, and inversely, the imaginary part of refractive indices increases. These phenomena can be explained by the physical mechanism of interaction between light and aerosols.

The RH is a major factor that affects aerosol size distribution, light scattering coefficients, and refractive index. In addition, there are also other impact factors such as chemical composition and particles size. With the change of the RH, the surface of aerosol particles may be adhered to by more chemical substances and water, which will cause a great change of the complex refractive indices. At the same time, the chemical composition and size change with space–time, and thus the imaginary index increases with the RH sometimes. This condition includes internal mixing and external mixing of aerosol, whose

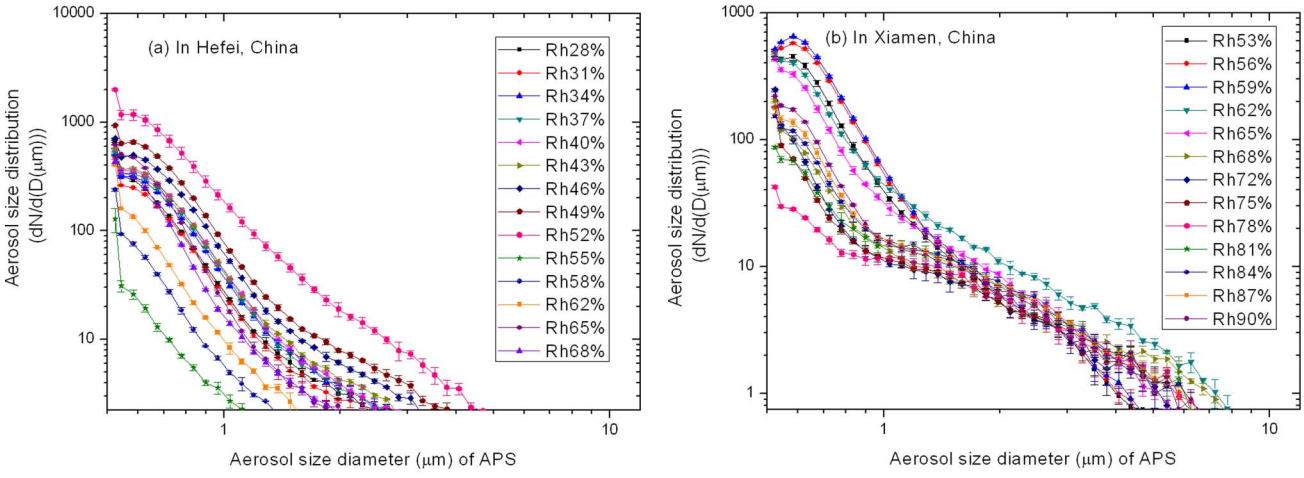

Fig. 7. (Color online) Aerosol size distributions at different values of RH measured (a) in Hefei and (b) in Xiamen, China, respectively.

optical properties are also complex. We consider that the further measurements of aerosol chemical composition and spectral character will increase accuracy of the complex refractive indices. The physical, chemical, and optical properties of aerosol particles were given by Gwaze *et al.* [73]. Biswas and Wu also showed a comparatively detailed summary on aerosol particles in the environment and policy [74].

C. Error Analysis

Careful inspection of Eq. (2) reveals several potential sources of errors in the retrieval of the complex refractive index. First, the APS only detects particles from 0.5 to 20 μm in diameter. Contribution to light scattering of any particles outside this APS diameter range would be counted in the nephelometer measurement, but not in the light scattering

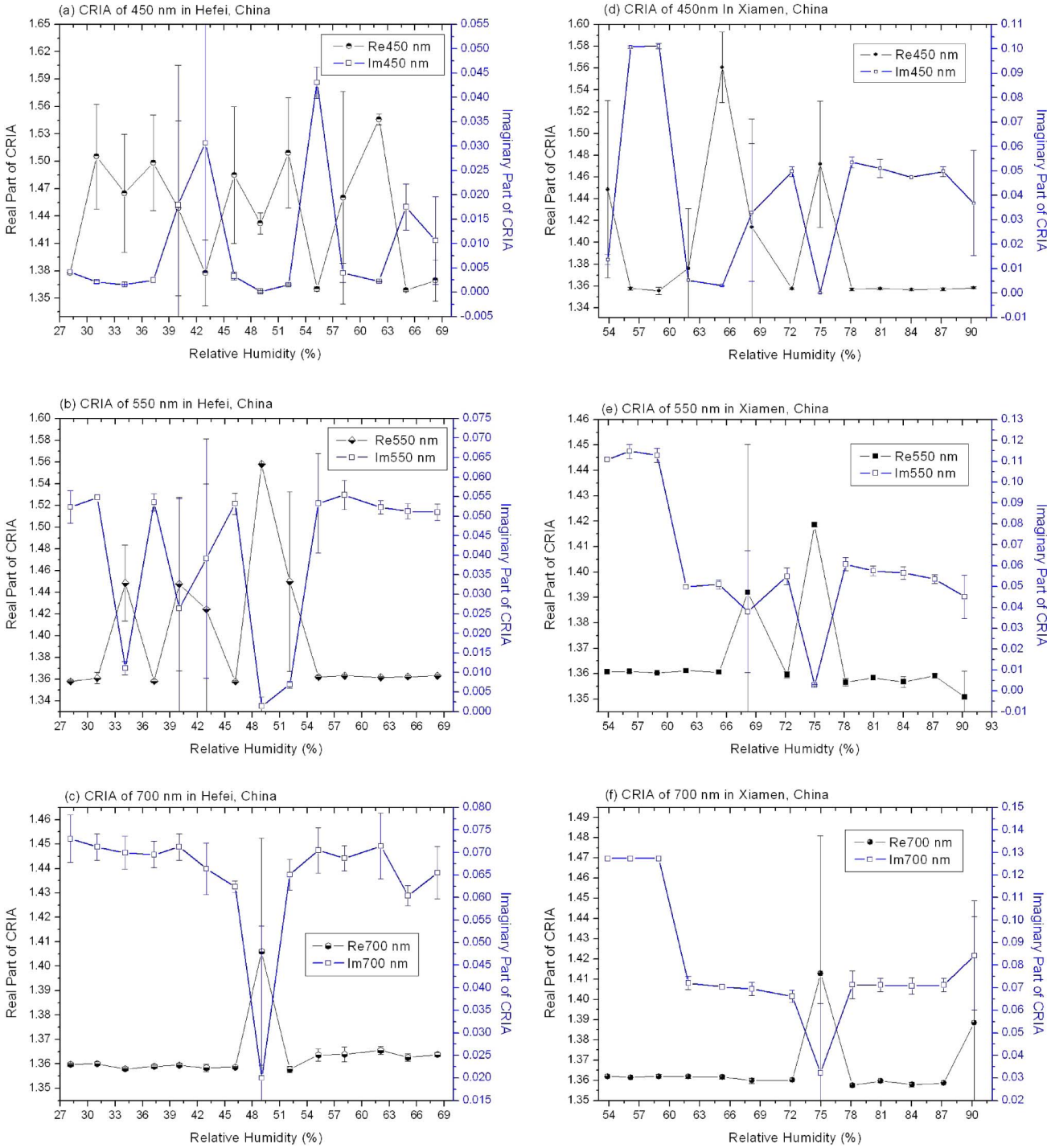

Fig. 8. (Color online) Refractive index as a function of RH. (a), (b), (c) Changes of the real and imaginary parts of the refractive indices at wavelengths 450, 550, and 700 nm in Hefei. (d), (e), (f) Changes of the real and imaginary parts of the refractive indices at wavelengths 450, 550, and 700 nm in Xiamen.

coefficients calculated from the APS-measured size distribution, leading to some size truncation error. Especially, the contribution from particles smaller than 0.5 μm could be noticeable as the sizes of these particles are comparable to the wavelengths of the nephelometer. To obtain some insight into this issue, Fig. 9 shows an example of combined aerosol size distributions (the RH was 77.6%) measured with the APS and SMPS probes at 15:15 pm on 4 October 2005 in Xiamen of China. At the same time, the aerosol total scattering coefficients are 5.485E-5, 4.576E-5, and 3.976E-5 $1/m$ for 450, 550, and 700 nm, respectively. By using the approach mentioned in Section 2, the retrieval is realized by an iterative least squares minimization of the fractional error between the nephenometer-measured light scattering coefficients and those calculated from the summation of SMPS-APS measured size distributions based on the Mie theory. So, using this combined size distribution, we estimated that the relative contributions of particles smaller than 0.5 μm to the real and imaginary parts are 6.07%, 11.11%, 0.73%, and 34.69%, 44.66%, 20.38% for 450, 550, and 700 nm, respectively, which shows that the relative contributions of particles smaller than 0.5 μm to the real part are smaller than those to the imaginary part. Further study is needed to see whether this property is in other space–time. Also noted is that the APS probe may suffer from the problem of counting efficiency [39].

Second, the APS probe measures the aerodynamic size that depends on the particle mass density as well. Any density difference between the ambient aerosol particles and the polystyrene particles used in the APS calibration will result in some error in the APS-measured size distributions, and hence the retrieved refractive index. Furthermore, it has been recently demonstrated that aerosol mass density and refractive index are likely related to each other, both depending on the chemical composition of the aerosol particle [38]. But, assessment of the density effects on the APS-measured size distributions and the refractive index is beyond the scope of this paper. Another relevant issue is the geometrical shape of the aerosol particle, which is not necessarily spherical as assumed in this work. Studies have shown that particle shape, refractive index, and size distributions are often mingled together in retrievals based on optical measurements (for details, see Ref. [75]). Of course, any sampling errors of the nephelometer will lead to errors in the retrieved refractive index as well [46–50].

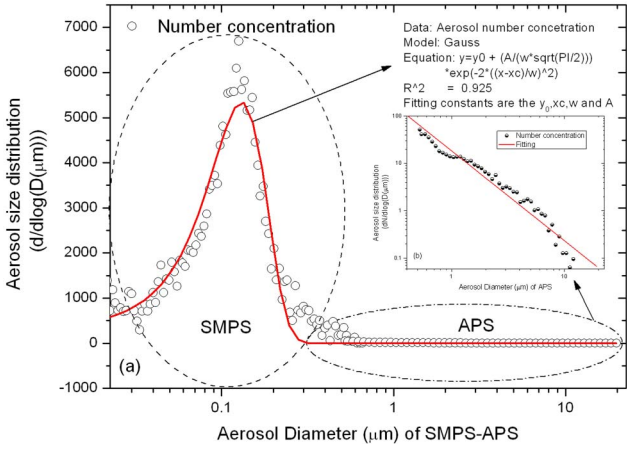

Fig. 9. (Color online) Aerosol size distribution for the data measured at 3:15 pm on 4 October 2005 in Xiamen, China.

4. Conclusions

An approach is developed to retrieve the complex index of refraction by coupling two well known instruments: an ASP probe for measuring aerosol size distributions and an integrating nephelometer for measuring total light scattering coefficients. The retrieval is realized by an iterative least squares minimization of the fractional error between the nephelometer-measured light scattering coefficients and those calculated from the ASP-measured size distributions based on the Mie theory for spherical particles. The approach has the advantages of easy implementation and high sampling frequency, and has been applied to the field experiments conducted at two locations with different environmental conditions in China (Hefei and Xiamen) in 2005.

Analyses of the time series of light scattering coefficients, aerosol size distributions, and refractive indices show that all three quantities vary substantially with time. Further examination of their dependence on RH suggests a complex picture. For example, instead of being monotonic change with RH, the refractive index often fluctuates when the RH changes. This nonmonotonic variation of refractive index with relative index suggests concurrent change of RH and other chemical compositions. Possible errors in the retrieval are also discussed. Future research will center around eliminating these errors by integrating measurements of particle shape, chemical compositions, and mixing states of ambient aerosols.

This work was jointly supported by the National Natural Science Foundation of China (NSFC#) (grant 40805006), the Science Foundation of the Key Laboratory of the Atmospheric Optics of the National High Technology Research and Development Program (863) of China (grant 2008-01), and the National Science Foundation for Postdoctoral Scientists of China (grant 20080440064). We are grateful to Dr. Xuejuan Ren (School of Atmosphere, Nanjing University) and Dr. Xiangao Xia (Institute of Atmospheric Physics, Chinese Academy of Sciences) for their help in the English usage of our initial manuscript. Especially, the authors are very grateful to Dr. Yangang Liu of the Brookhaven National Laboratory, USA, and the anonymous reviewers for their insightful comments.

References

1. R. J. Charlson, J. E. Lovelock, M. O. Andreae, and S. G. Warren, "Oceanic phytoplankton, atmospheric sulphur, cloud albedo, and climate," Nature **326**, 655–661 (1987).
2. X. Zhou, S. Tao, and K. Yao, *Advanced Atmospheric Physics* (Meteorology Publishing House, 1991).
3. D. A. Hegg, P. V. Hobbs, S. Gasso, J. D. Nance, and A. L. Rangno, "Aerosol measurements in the Arctic relevant to direct and indirect radiative forcing," J. Geophys. Res. **101**, 23349–23363 (1996).
4. Y. Liu and P. H. Daum, "Anthropogenic aerosols: indirect warming effect from dispersion forcing," Nature **419**, 580–581 (2002).
5. V. Ramanathan, P. J. Crutzen, J. T. Kiehl, and D. Rosenfeld, "Aerosols, climate, and the hydrological cycle," Science **294**, 2119–2124 (2001).
6. J. Liu and J. Diamond, "China's environment in a globalizing world," Nature **435**, 1179–1186 (2005).
7. Y. Han, T. Wang, R. Rao, and Y. Wang, "The research progress on physic-optics characteristics of atmospheric aerosol," Acta Phys. Sin. **57**, 7396–7407 (2008) (in Chinese).
8. C. Xie, T. Nishizawa, N. Sugimoto, I. Matsui, and Z. F. Wang, "Characteristics of aerosol optical properties in pollution and Asian dust episodes over Beijing, China," Appl. Opt. **47**, 4945–4951 (2008).
9. J. L. Machol, R. D. Marchbanks, C. J. Senff, B. J. McCarty, W. L. Eberhard, W. A. Brewer, R. A. Richter, R. J. Alvarez, D. C. Law, A. M. Weickmann, and S. P. Sandberg, "Scanning tropospheric ozone and aerosol lidar with double-gated photomultipliers," Appl. Opt. **48**, 512–524 (2009).
10. S. J. Ghan and S. E. Schwartz, "Aerosol properties and processes: a path from field and laboratory measurements to global climate models," Bull. Am. Meteorol. Soc. **88**, 1059–1083 (2007).
11. C. H. Chan, "Effective absorption for thermal blooming due to aerosols," Appl. Phys. Lett. **26**, 628–629 (1975).
12. F. G. Gebhardt, "High power laser propagation," Appl. Opt. **15**, 1479–1493 (1976).
13. C. F. Bohren and D. R. Huffman, *Absorption and Scattering of Light by Small Particles* (Wiley-Interscience, 1983), pp. 28–30.
14. V. B. Krapchev, "Atmospheric thermal blooming and beam clearing by aerosol vaporization," Proc. SPIE **1221**, 91–105 (1990).
15. X. Yang, J. Wang, Y. Liu, and D. Wan, "Aerosol induced air breakdown with Nd:YAG pulsed laser radiation," High Power Laser Particle Beams **9**, 157–160 (1997) (in Chinese).
16. L. Y. Chen, M. C. Chou, L. K. Hwang, W. Y. Lin, C. C. Chen, and F. T. Jeng, "Aerosol scattering coefficients at different humidities," J. Aerosol Sci. **31** (suppl.), 983–984 (2000).
17. K. N. Liou, *An Introduction to Atmospheric Radiation*, 2nd ed. (Elsevier, 2002).
18. G. Yamamoto and M. Tanaka, "Increase of global albedo due to air pollution," J. Atmos. Sci. **29**, 1405–1412 (1972).
19. V. Ramanathan, M. V. Ramana, G. Roberts, D. Kim, C. Corrigan, C. Chung, and D. Winker, "Warming trends in Asia amplified by brown cloud solar absorption," Nature **448**, 575–578 (2007).
20. R. Eiden, "Determination of the complex index of refraction of spherical aerosol particles," Appl. Opt. **10**, 749–754 (1971).
21. C. I. Lin, M. Baker, and R. J. Charlson, "Absorption coefficient of atmospheric aerosol: a method for measurement," Appl. Opt. **12**, 1356–1363 (1973).
22. M. Z. Hansen and W. H. Evans, "Polar nephelometer for atmospheric particulates studies," Appl. Opt. **19**, 3389–3395 (1980).
23. F. Zhao, Z. Gong, H. Hu, and M. Tanaka, "Simulataneous determination of the aerosol complex index of refraction and size distribution from scattering measurements of polarized light," Appl. Opt. **36**, 7992–8001 (1997).
24. F. Zhao, "Determination of complex index of refraction and size distribution of aerosols from polar nephelometer measurements," Appl. Opt. **38**, 2331–2336 (1999).
25. P. Romanov, N. T. O'Neill, A. Royer, and Bruce L. J. McArthur, "Simultaneous retrieval of aerosol refractive index and particle size distribution from ground-based measurements of direct and scattered solar radiation," Appl. Opt. **38**, 7305–7320 (1999).
26. W. Tian and C. Chen, "Parameterization of optical characteristics of aerosols over Lanzhou city in winter," Sci. Atmos. Sin. **20**, 235–242 (1996) (in Chinese).
27. W. Tian, C. Chen, and J. Huang, "Spectral character and complex refractive index of the winter aerosol over Lanzhou city," J. Lanzhou Univ. **32**, 126–132 (1996).
28. Q. Guo, H. Hu, and J. Zhou, "Measurement of elemental carbon in the atmospheric aerosol and correlation with its imaginary refractive index," Sci. Atmos. Sin. **20**, 633–639 (1996). (in Chinese)
29. Y. Liu and P. H. Daum, "The effect of referactive index on size distributions and light scattering coefficients derived from optical particle counters," J. Aerosol Sci. **31**, 945–957 (2000).
30. P. Guyona, O. Boucher, B. Graham, J. Beck, O. Mayol-Bracero, G. Robertsa, W. Maenhaut, P. Artaxoe, and M. Andreae, "Refractive index of aerosol particles over the Amazon tropical forest during LBA-EUSTACH 1999," J. Aerosol Sci. **34**, 883–907 (2003).
31. J. L. Hand and S. M. Kreidenweis, "A new method for retrieving particle refractive index and effective density from aerosol size distribution data," Aerosol Sci. Technol. **36**, 1012–1026 (2002).
32. H. Hu, X. Li, Y. Zhang, and T. Li, "Determination of the refractive index and size distribution of aerosol from dual-scattering-angle optical particle counter measurements," Appl. Opt. **45**, 3864–3870 (2006).
33. Y. Liu and P. H. Daum, "Relationship of refractive index to mass density and self-consistency of mixing rules for multicomponent mixtures like ambient aerosols," J. Aerosol Sci. **39**, 974–986 (2008).
34. K. M. Adams, "Real-time in situ measurements of atmospheric optical absorption in the visible via photoacoustic spectroscopy. 1. Evaluation of the photoacoustic cells," Appl. Opt. **27**, 4052–4056 (1988).
35. P. H. McMurray, "A review of atmospheric aerosol measurements," Atmos. Environ. **34**, 1959–1999 (2000).
36. H. Hu, J. Xu, and Z. Huang, "The characteristics of the imaginary part of aerosol refractive index in some places of eastern China," Chin. J. Atmos. Sci. **15**, 18–23 (1991). (in Chinese)
37. J. C. Wilson and B. Liu, "Aerodynamic particle size measurement by laser-doppler velocimetry," J. Aerosol Sci. **11**, 139–150 (1980).
38. T. Nakajima, M. Tanaka, M. Yamano, M. Shiobara, K. Arao, and Y. Nakanishi, "Aerosol optical characteristics in the yellow sand events observed in May, 1982 at Nakasaki. II. Models," J. Meteorol. Soc. Jpn. **67**, 279–291 (1989).
39. T. M. Peters and D. Leith, "Concentration measurement and counting efficiency of the aerodynamic particle sizer 3321," J. Aerosol Sci. **34**, 627–634 (2003).
40. J. K. Agarwal, G. J. Sem, and R. J. Remiaz, "Filter testing with a continuous-flow, single-particle-counting condensation nucleus counter," TSI Quarterly 11, 3–12 (1985).
41. J. Shi, R. M. Harrison, and D. Evans, "Comparison of ambient particle surface area measurement by epiphaniometer and SMPS/APS," Atmos. Environ. **35**, 6193–6200 (2001).
42. S. Shen, P. A. Jaques, Y. Zhu, M. D. Geller, and C. Sioutas, "Evaluation of the SMPS–APS system as a continuous monitor for measuring $PM_{2.5}$, PM_{10} and coarse ($PM_{2.5-10}$) concentrations," Atmos. Environ. **36**, 3939–3950 (2002).

43. A. Virkkula and R. E. Hillamo, "Three-wavelength nephelometer measurements in the Finnish arctic," J. Aerosol Sci. **26** (suppl.), S451–S452 (1995).
44. T. R. Muraleedharan and M. Radojevic, "Personal particle exposure monitoring using nephelometry during haze in Brunei," Atmos. Environ. **34**, 2733–2738 (2000).
45. R. G. Beuttell and A. W. Brewer, "Instruments for the measurement of the visual range," J. Sci. Instrum. **26**, 357–359 (1949).
46. R. J. Charlson and N. C. Ahlquist, "Integrating nephelometer," U.S. patent 3563661 (16 February 1971).
47. B. A. Bodhalne, "Measurement of the Rayleigh scattering properties of some gases with a nephelometer," Appl. Opt. **18**, 121–125 (1979).
48. M. Z. Hansen and W. H. Evans, "Polar nephelometer for atmospheric particulates studies," Appl. Opt. **19**, 3389–3395 (1980).
49. J. B. Rae and J. A. Garland, "A stabilized integrating nephelometer for visibility studies," Atmos. Environ. **4**, 219–223 (1970).
50. J. Heintzenberg and L. Backlin, "A height sensitivity integration nephelometer for airborne air pollution," Atmos. Environ. **17**, 433–436 (1983).
51. B. A. Bodhaine, "Aerosol measurements at four background sites," J. Geophys. Res. **88**, 10753 (1983).
52. M. J. Rood, D. S. Covert, and T. V. Larson, "Hygroscopic properties of atmospheric aerosol in Riverside, California," Tellus **39B**, 383–397 (1987).
53. B. A. Bodhaine, "Barrow surface aerosol: 1976–1986," Atmos. Environ. **23**, 2357–2369 (1989).
54. B. A. Bodhaine, J. M. Harris, and G. A. Herbert, "Aerosol light scatting and condensation nuclei measurements at Barrow, Alaska," Atmos. Environ. **15**, 1375–1389 (1981).
55. M. J. Rood, M. A. Shaw, T. V. Larson, and D. S. Covert, "Ubiquitous nature of ambient metastable aerosol," Nature **337**, 537–539 (1989).
56. B. A. Bodhaine, C. N. Ahlquist, and R. C. Schenell, "Three-wavelength nephelometer suitable for aircraft measurement of background aerosol scattering coefficient," Atmos. Environ. **A25**, 2267–2276 (1991).
57. R. J. Charlson, S. E. Schwartz, J. M. Hales, R. D. Cess, J. A. Coakley, J. E. Hansen, and D. J. Hofmann, "Climate forcing by anthropogenic aerosols," Science **255**, 423–430 (1992).
58. J. P. Veefkind, J. C. H. van der Hage, and H. M. ten Brink, "Nephelometer derived and directly measured aerosol optical depth of the atmospheric boundary layer," Atmos. Res. **41**, 217–228 (1996).
59. F. Li, S. Nyeki, U. Baltensperger, E. Weingartner, M. Lugauer, I. Colbeck, and H. W. Giiggeler, "Aerosol size distribution retrieval from multi-wavelength nephelometer data," J. Aerosol Sci. **28** (suppl.), S249–S250 (1997).
60. S. A. P. Nyecki, I. Colebeck, and R. M. Harrison, "A portable aerosol sampler to measure real-time atmospheric aerosol mass loadings," J. Aerosol Sci. **23**, S687–S690 (1992).
61. A. D. Shendrikar and W. K. Steinmetz, "Integrating nephelometer measurements for the airborne fine particulate matter (PM2.5) mass concentrations," Atmos. Environ. **37**, 1383–1392 (2003).
62. K. Werner, "A new polar nephelometer for measurement of atmospheric aerosols," J. Quant. Spectrosc. Radiat. Transfer **87**, 107–117 (2004).
63. B. Hu, W. Zhang, L. Zhang, C. Chen, and G. Feng, "A study on scattering properties of aerosol particle over Xigu district of Lanzhou," Plateau Meteorol. **22**, 354–360 (2003) (in Chinese).
64. Z. Ke, J. Tang, B. Wang, and P. Yang, "Primary analysis of application results of integrating nephelometers in dust storm monitoring network experiment," Meteorol. Sci. Technol. **32**, 258–262 (2004) (in Chinese).
65. B. Hu, J. Zhang, W. Zhang, C. Chen, and L. Zhang, "A study of the properties of atmospheric aerosol over Lanzhou in winter and applications by using integrating nephelometer," J. Lanzhou Univ. **41**, 9–25 (2005) (in Chinese).
66. Y. Han, "Measurements and statistical characteristics of atmospheric aerosol optical properties," Ph.D dissertation (Anhui Institute of Optics and Fine Mechanics, 2006) (in Chinese).
67. Y. Han, R. Rao, and Y. Wang, "Measurement and analysis of atmospheric visibility and aerosol extinction characteristics based on scattering statistical," Infrared Laser Eng. **4**, 663–666 (2008) (in Chinese).
68. G. Mie, "Beitrage zur optik trüber medien, spezielle kolloidaller metallosungen," Ann. Phys. **25**, 377–444 (1908).
69. W. J. Wiscombe, "Mie scattering calculations: advances in technique and fast, vector-speed computer codes," Technical Note NCAR/TN-140+STR (National Center for Atmospheric Research, June 1979).
70. W. J. Wiscombe, "Improved Mie scattering algorithms," Appl. Opt. **19**, 1505–1509 (1980).
71. V. E. Cachorro and L. L. Salcedo, "New improvements for Mie scattering calculations," J. Electromagn. Waves Appl. **5**, 913–926 (1991).
72. W. Wang and M. J. Rood, "Real refractive index: dependence on relative humidity and solute composition with relevancy to atmospheric aerosol particles," J. Geophys. Res. **113**, D23305 (2008).
73. P. Gwaze, G. Helas, H. J. Annegarn, J. Huth, and S. J. Piketh, "Physical, chemical and optical properties of aerosol particles collected over Cape Town during winter haze episodes," S. Afr. J. Sci. **103**, 35–43 (2007).
74. P. Biswas and C. Y. Wu, "Nanoparticles and the environment," J. Air Waste Manag. Assoc. **55**, 708–746 (2005).
75. Y. Liu, W. P. Arnott, and J. Hallett, "Particle size distribution retrieval from multispectral optical depth: influences of particle nonsphericity and refractive index," J. Geophys. Res. **104**, 31753–31762 (1999).